EPJ D
Atomic, Molecular, Optical and Plasma Physics
EPJ.org
your physics journal

Eur. Phys. J. D (2013) 67: 251 DOI: 10.1140/epjd/e2013-40567-5

Structural stability, chemical order and reactivity pattern of Mo_pW_q clusters, with $p + q = 8$

Reinaldo Pis-Diez and Faustino Aguilera-Granja

edp sciences
Società Italiana di Fisica
Springer

Eur. Phys. J. D (2013) 67: 251
DOI: 10.1140/epjd/e2013-40567-5

THE EUROPEAN PHYSICAL JOURNAL D

Regular Article

Structural stability, chemical order and reactivity pattern of Mo_pW_q clusters, with p + q = 8

Reinaldo Pis-Diez[1,a] and Faustino Aguilera-Granja[2]

[1] CEQUINOR, Centro de Química Inorgánica (CONICET, UNLP) Departamento de Química, Facultad de Ciencias Exactas, UNLP C.C. 962, 1900 La Plata, Argentina
[2] Instituto de Física "Manuel Sandoval Vallarta", Universidad Autónoma de San Luis Potosí, S.L.P. 78000, Mexico

Received 11 September 2013 / Received in final form 11 October 2013
Published online 10 December 2013 –

Abstract. The electronic structure and related properties of free-standing Mo_pW_q atomic clusters, with $p+q=8$, are investigated within the framework of the fully unconstrained version of the density functional theory as implemented in the SIESTA code. Starting from the structures of the lowest-energy isomers of pure Mo_8 and W_8, they are decorated for any possible homotops and their geometries are re-optimized. Binding energies, excess energies and second differences in binding energies are reported and used to discuss relative stabilities of different isomers. Interatomic distances, magnetic moments, average coordination numbers and order parameters are also reported to achieve a better understanding of the structural evolution of the species when Mo atoms are replaced by W atoms and vice versa. Adiabatic ionization potentials, adiabatic electronic affinities and absolute hardnesses are also shown and discussed in the context of the potential reactivity of Mo_pW_q clusters against hydrotreatment processes. Those reactivity indexes suggest that the Mo_3W_5 aggregate should be a good candidate to take part in a reaction governed by a charge transfer process.

1 Introduction

Catalysts based on molybdenum and tungsten play an important role in the petroleum industry. Owing to their resistance to poisons, those systems are unique catalysts for the removal of heteroatoms (N, S, O) in the presence of large amounts of hydrogen. Hydrodesulfurization (HDS), the removal of sulfur from organic molecules, such as thiophene and benzothiophene, present in crude oils is generally performed with molybdenum or tungsten sulfides supported on alumina [1]. The catalytic activity of these sulfides is often enhanced with cobalt or nickel for the HDS process [2–4].

NiW sulfide catalysts have not been used as frequently as CoMo and NiMo sulfide catalysts in hydrotreatments (HDT), because W-based catalysts are difficult to convert to sulfides and also because they are less active than Mo-based catalysts for the HDS process [5]. However, the W-based catalysts are an interesting option for hydrodenitrogenation (HDN), the removal of nitrogen from petroleum feedstocks [6,7].

There have been various attempts to improve the catalytic performance of the conventional Ni(Co)Mo hydrotreating catalyst. Interestingly, an attempt by incorporating a small amount of tungsten into Ni(Co)Mo catalysts was proved to have a promoting effect on the HDS and hydrogenation (HYD) activities [8–10]. Lee et al. suggested that the relatively low content of tungsten on the Ni(Co)Mo/γ-Al_2O_3 catalysts facilitates the reduction of Mo-O species and increases the dispersion of MoS_2 [8,9]. However, Vakros and Kordulis proposed that the increase in the HDS activity of the Ni(Co)Mo/γ-Al_2O_3 catalysts after the addition of a small amount of tungsten is due to a simple increase in the total active phase, while the increase in the HYD activity is assigned to the higher activity of the W-phase [10].

Nowadays the potential application of NiMoW catalysts for HDT has been explored and it has been reported that when Mo is partially substituted by W, an amorphous phase is created, which after reduction and sulfidation produces catalytically active materials [1,11–13].

Nanoclusters are aggregates that can present from a few to many millions of atoms or molecules. The current interest in nanocluster science arises because these aggregates are a new type of material, whose properties differ both from those of isolated atoms or molecules and from those of bulk materials. Interestingly, those unique properties can be studied in different media such as the vapor phase or on surfaces [14]. For this reason, transition metal (TM) clusters, both free and supported, constitute an exciting alternative to the classical catalysts [15].

[a] e-mail: pis_diez@quimica.unlp.edu.ar

A natural starting point for understanding the properties of TM clusters is the determination of their geometries, since most of their physical and chemical properties are strongly related to structural features. Experimental information on the geometries of TM clusters can be acquired by several means, including the chemical probe method, in which the cluster structure is inferred from the level of the adsorption of molecules such as N_2 onto the cluster surface [16–20]. However, experimental determinations are not always unequivocal, and, in these cases, the elucidation of structures can be aided by computer simulations based on appropriate theoretical models.

Determining the geometry of TM clusters using computational tools is a nontrivial task, however, due to the numerous d electrons present in the system. These electrons give rise to many electronic states, very close in energy, that compete to be the ground state for different geometries. In the case of a binary system, one additional characteristic must be considered besides the problem in the determination of the geometrical and electronic structures. Finding the chemical order or composition of each cluster of every size is mandatory to achieve a complete description of the system.

Small molybdenum clusters up to about 13 atoms have been thoroughly investigated in the last decade using several methodologies, most of those based on the density functional theory, see for example references [21,22] and publications cited therein. Tungsten clusters, on the other hand, were apparently less studied and, as a consequence of this, some few reports are found in the literature [23–26]. The most recent studies were devoted to investigate the properties of W clusters up to about 20 atoms [25,26].

The aim of this contribution is to discuss a possible connection between the HDT activity of Mo-, W- and MoW-based catalysts, on the one hand, and the geometric and electronic structures and chemical order presented in small MoW clusters, on the other hand. It has been reported that small Mo clusters grow according to 1D and 2D patterns from the dimer up to the heptamer, whereas larger clusters exhibit 3D patterns when growing [22]. This is not the case of W clusters, for which the 3D pattern is already present in the tetramer [26]. Thus, clusters having eight atoms are the smallest systems in which both structures show a 3D growing pattern. To the best of our knowledge, this is the first computational study on this nanoalloy formed by molybdenum and tungste with up to eight atoms. The rest of the paper is organized as follows. In Section 2 the computational approach used in this contribution is described. Interatomic distances, binding energies, magnetic moments, ionization energies, electron affinities and other structural features of Mo_pW_q clusters, with $p + q = 8$, are reported and discussed in Section 3. Finally, the main conclusions are summarized in Section 4.

2 Computational details

The geometrical and electronic structure, the chemical order and the magnetic properties of free-standing Mo_pW_q clusters, with $p + q = 8$, were obtained using the SIESTA program, in which the single particle Kohn-Sham equations are solved in a numerical pseudoatomic orbitals basis set [27]. The atomic cores were described by nonlocal, norm-conserving Troullier-Martins pseudopotentials [28]. The pseudopotentials are factorized in the Kleinman-Bylander form [29]. The pseudopotentials for Mo and W were generated using the $5s^1 4d^5 5p^0$ and $6s^2 5d^4 6p^0$ valence configurations, respectively. The cut-off radii for the d, s and p states were 1.67 a.u., 2.30 a.u. and 2.46 a.u. for Mo, and 2.24 a.u., 2.85 a.u. and 3.03 a.u. for W, respectively. The core corrections were included using a radius of 1.20 a.u. and 1.30 a.u. for Mo and W, respectively. The valence states were described by a double-ζ basis set augmented with two sets of polarization functions, DZ2P from now on. Some tests were carried out with a triple-ζ basis set augmented with two sets of polarization functions, TZ2P, see Table 1. The energy cut-off used to define the real-space grid for the numerical calculations involving the electron density was 250 Ry. The gradient-corrected functional due to Perdew, Burke and Ernzerhof was used to reproduce exchange and correlation effects [30]. All the calculations were performed in the free-spin mode. This usually provides the most stable spin-isomer in the case of ferromagnetic-like clusters. Additional calculations in the fixed-spin mode were carried out for those spin states adjacent to the most stable spin states obtained as above, to ensure that these correspond to the most stable spin configurations.

The bimetallic clusters were placed in a $20 \times 20 \times 20$ Å^3 supercell, which is large enough both for considering negligible any interaction between the cluster and its replicas in neighboring cells, and for considering only the Γ point ($k = 0$) when integrating over the Brillouin zone. All the starting structures were fully relaxed following a conjugate gradient method [31] without any geometry constrains until the interatomic forces were smaller than 0.006 eV/Å.

Table 1. Comparison of experimental and calculated values of binding energy, E_b in eV/at, and equilibrium distance, R_e in Å, for gas phase dimers and bulk systems. Calculated values in the present work correspond to PBE/DZ2P and PBE/TZ2P levels of theory.

	E_b	R_e	E_b	R_e
	Mo_2		Mo (bulk)	
PBE/DZ2P	–1.998	1.712	–5.281	2.763
PBE/TZ2P	–2.209	1.657	–5.956	2.738
Exp. [35,36]	2.19 ± 0.05	1.80–2.10	–6.820	2.725
	W_2		W (bulk)	
PBE/DZ2P	–2.599	1.835	–8.243	2.760
PBE/TZ2P	–2.711	1.815	–8.406	2.760
Exp. [35,36]	2.50 ± 0.50	2.155–2.264	–8.900	2.741
	MoW		MoW (bulk)	
PBE/DZ2P	–2.543	1.760	–6.940	2.753
PBE/TZ2P	–2.760	1.712	–7.253	2.744

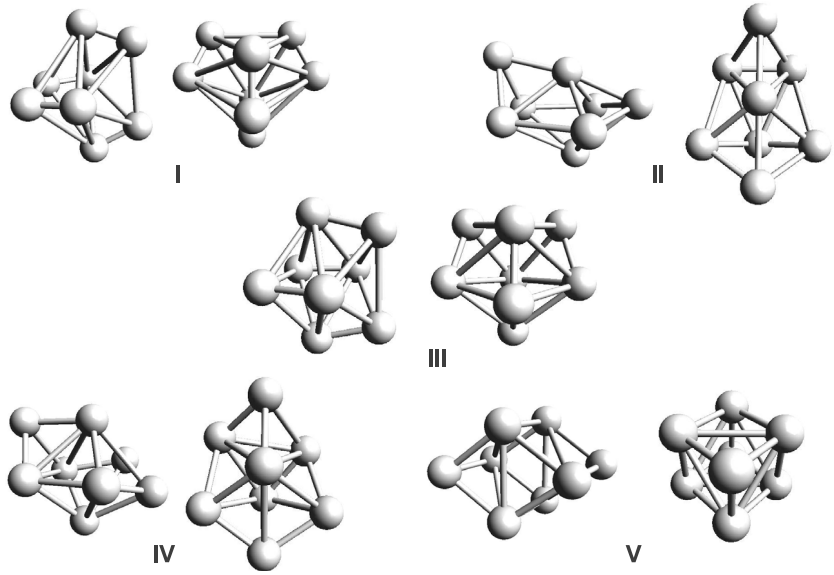

Fig. 1. Two different views of the starting geometries considered in the present work. Isomer I is the lowest-energy structure of Mo_8. Isomer V is the lowest-energy structure of W_8.

The search of lower-energy homotops of Mo_pW_q clusters, with $p+q=8$, was conducted as follows. We started with the five lower-energy isomers of pure Mo_8 and W_8, which are represented in Figure 1. The dodecaedral structure, isomer I from now on, is the lowest-energy isomer of Mo_8 [22] and the fourth lowest-energy isomer of W_8 [26]. The thin decaedral isomer, isomer II from now on, is very close in energy to the ground state (GS) of Mo_8 and is the fifth isomer in the case of W_8. The decaedral, octahedral and parallelepiped forms, isomers III, IV and V from now on, respectively, are higher in energy with respect to the GS in the case of Mo_8. On the other hand, isomer V is the GS of W_8, whereas isomers III and IV are very close in energy to the GS.

The second step in the present procedure was to optimize the geometry with respect to the total energy of all possible Mo_7W initial configurations resulting from the substitution of a Mo atom by a W atom in all the inequivalent sites for each one of the geometries shown in Figure 1. Then, the three lowest-energy homotops of these Mo_7W isomers for each one of the five initial geometries are selected and a new Mo atom is substituted by a W atom, considering all the inequivalent sites, thus generating a series of Mo_6W_2 aggregates. The geometries of those aggregates are optimized and, again, the three lowest-energy homotops of each starting Mo_6W_2 are selected to generate new starting geometries for Mo_5W_3. This procedure was repeated until the equiatomic Mo_4W_4 stoichiometry is reached. Next, the same procedure was carried out starting with the five pure W_8 isomers shown in Figure 1 and replacing W atoms one at a time until the Mo_4W_4 stoichiometry is reached.

The relative stability of a given Mo_pW_q cluster is evaluated by means of the binding energy, which is calculated as:

$$E_b(\mathrm{Mo}_p\mathrm{W}_q) = \frac{E_{\mathrm{Mo}_p\mathrm{W}_q} - pE_{\mathrm{Mo}} - qE_{\mathrm{W}}}{8}, \qquad (1)$$

where $E_{\mathrm{Mo}_p\mathrm{W}_q}$ is the total electronic energy of the Mo_pW_q aggregate and E_{Mo} and E_{W} are the total electronic energies of the atoms in their corresponding GS. Negative binding energies indicate that the aggregate is more stable than the isolated atoms. On the other hand, to determine whether the formation of a given Mo_pW_q aggregate is favorable with respect to the pure clusters, Mo_8 and W_8, the concept of excess energy is used [32]. The excess energy is defined as:

$$E'_{exc}\left(\mathrm{Mo}_p\mathrm{W}_q\right) = E_{\mathrm{Mo}_p\mathrm{W}_q} - \frac{p}{8}E_{\mathrm{Mo}_8} - \frac{q}{8}E_{\mathrm{W}_8}, \qquad (2)$$

where E_{Mo_8} and E_{W_8} stand for the total electronic energy of pure clusters in their global GS. Equation (2) can be written in terms of binding energies as:

$$E_{exc}\left(\mathrm{Mo}_p\mathrm{W}_q\right) = E_b\left(\mathrm{Mo}_p\mathrm{W}_q\right) - \frac{p}{8}E_b\left(\mathrm{Mo}_8\right) - \frac{q}{8}E_b\left(\mathrm{W}_8\right), \qquad (3)$$

in which $E_{exc} = E'_{exc}/8$. According to the present definition of binding energy, a negative value of E_{exc} indicates that the formation of the binary cluster is favored with respect to pure aggregates. As the present study deals with the different homotops derived from a given starting structure, isomers I to V shown in Figure 1, it could be more useful to define the excess energy in terms of the binding energies of those pure clusters of the same isomer instead of using the global GS.

To compare the relative stability of binary clusters of nearby composition, the second difference in the binding energy can also be used [32]

$$\Delta_2 E\left(\mathrm{Mo}_p\mathrm{W}_q\right) = E_b\left(\mathrm{Mo}_{p+1}\mathrm{W}_{q-1}\right) + E_b\left(\mathrm{Mo}_{p-1}\mathrm{W}_{q+1}\right) - 2E_b\left(\mathrm{Mo}_p\mathrm{W}_q\right), \qquad (4)$$

where the binding energies correspond to the most stable clusters of each composition. Thus, positive values of

$\Delta_2 E(\mathrm{Mo}_p\mathrm{W}_q)$ indicate that the given cluster is more stable than its two immediate neighbors.

The ionization energy (IE) and the electron affinity (EA) are defined as:

$$\mathrm{IE} = E_{\mathrm{Mo}_p\mathrm{W}_q^+} - E_{\mathrm{Mo}_p\mathrm{W}_q} \tag{5}$$

and

$$\mathrm{EA} = E_{\mathrm{Mo}_p\mathrm{W}_q} - E_{\mathrm{Mo}_p\mathrm{W}_q^-}. \tag{6}$$

As the geometry of the charged species is allowed to relax after the electron is added or removed, the above quantities are better called adiabatic IE (AIE) and adiabatic EA (AEA).

As a measure of the potential reactivity of a given species in a charge transfer process, the global hardness, η, can be a useful, qualitative parameter [33]

$$\eta = \frac{\mathrm{AIE} - \mathrm{AEA}}{2}. \tag{7}$$

Systems with small values of hardness, that is, systems with small AIE and large AEA values, would have a great chance to participate in a charge transfer process.

Finally, it is worth noting that multi-component systems can be characterized by the tendency of the constituent elements to mix or segregate. Ducastelle introduced the concept of order parameter to analyze qualitatively those trends in the case of bulk-like binary alloy systems [34]

$$\sigma = \frac{N_{\text{A-A}} + N_{\text{B-B}} - N_{\text{A-B}}}{N_{\text{A-A}} + N_{\text{B-B}} + N_{\text{A-B}}}, \tag{8}$$

where $N_{\text{A-B}}$, for example, is the number of bonds formed by A and B. In bulk-like binary systems the parameter σ allows to make a clear distinction between two limiting situations, namely, segregation, in which $\sigma \approx 1$ on the one hand, and perfect mixing or disorder, in which $\sigma \approx -1$ on the other hand. In more realistic situations it is expected that $\sigma > 0$ in systems where segregation dominates, whereas values of $\sigma < 0$ would indicate some degree of mixing. In those small clusters, in which one of the components, say A, is clearly in excess with respect to the other, say B, the above order parameter fails to describe well the tendency of B to mix. This is due to the fact that even when $N_{\text{B-B}}$ is negligible or null, $N_{\text{A-A}}$ is still considerably larger to be the dominant part in equation (8). Then, σ will be greater than zero thus failing to describe the mixing tendency exhibited by B in diluted A-B clusters. To remedy this, it is proposed to consider an order parameter for each component in an $\mathrm{A}_p\mathrm{B}_q$ aggregate by simply separating equation (8) in two parts as:

$$\sigma_A = \frac{N_{\text{A-A}} - \frac{p}{p+q} N_{\text{A-B}}}{N_{\text{A-A}} + N_{\text{B-B}} + N_{\text{A-B}}}, \tag{9}$$

and

$$\sigma_B = \frac{N_{\text{B-B}} - \frac{q}{p+q} N_{\text{A-B}}}{N_{\text{A-A}} + N_{\text{B-B}} + N_{\text{A-B}}}, \tag{10}$$

where it is clear that $\sigma = \sigma_A + \sigma_B$. The weighting functions before the $N_{\text{A-B}}$ term are used to achieve a proper description for diluted systems, in which mixing is still observed. The individual order parameters, thus, can range from positive values when segregation dominates to negative values for disordered structures.

Table 2. Binding energy, E_b in eV/at, order parameters, σ_{Mo} and σ_{W}, average equilibrium distance, R_e^{avg} in Å, average coordination numbers, N_{Mo}^{avg} and $\mathrm{N}_{\mathrm{W}}^{avg}$, and magnetic moment, μ in μ_B, for aggregates derived from isomer I, see Figure 1 for the starting geometry and Figure 2 for labels.

Aggregate	E_b	σ_{Mo}	σ_{W}	R_e^{avg}	N_{Mo}^{avg}	N_{W}^{avg}	μ
I-a	–2.816	–	–	2.812	4.50	–	0.00
I-b	–2.982	0.48	–0.03	2.764	4.43	5.00	0.00
I-c	–3.235	0.17	–0.06	2.630	4.33	5.00	0.00
I-d	–3.471	0.11	0.00	2.620	4.40	4.67	0.00
I-e	–3.705	0.06	0.06	2.610	4.50	4.50	0.00
I-f	–3.927	–0.10	–0.01	2.585	4.67	4.40	0.00
I-g	–4.168	–0.13	0.13	2.583	4.50	4.50	0.00
I-h	–4.384	–0.03	0.48	2.584	5.00	4.43	0.00
I-i	–4.610	–	–	2.584	–	4.50	0.00

3 Results and discussion

Table 1 shows the comparison of selected calculated values and experimental data, when available, for the three possible dimers in the gas phase, Mo_2, W_2 and MoW, and for bulk Mo, W and MoW. As no experimental information was found for bulk MoW, a CsCl structure was used for the calculations. Two levels of theory were considered for testing purposes, differing only in the quality of the basis sets. The levels are labeled PBE/DZ2P and PBE/TZ2P, see Section 1 for details. It can be seen from the table that the binding energy of W_2 is well described by the two levels of theory. The binding energy of Mo_2, on the other hand, is underestimated by about 0.15–0.20 eV/at by the PBE/DZ2P level of theory but it is well described by the PBE/TZ2P one. On the contrary, the equilibrium distance of the homonuclear dimers exhibits a better agreement with experimental values for the PBE/DZ2P level of theory, with an appreciable decrease in its value when the quality of the basis set increases. For bulk Mo and W the binding energy is greatly underestimated by both levels of theory, whereas the equilibrium distance is slightly overestimated by both PBE/DZ2P and PBE/TZ2P. In the light of these results, the use of the PBE/DZ2P level of theory seems to be a good compromise between accuracy and speed of computation. This is an important issue considering the very large amount of isomers to be calculated for $\mathrm{Mo}_p\mathrm{W}_q$, with $p+q=8$. Thus, the PBE/DZ2P level of theory is used throughout.

Figure 2 shows the optimized structures of the most stable species for each composition derived from isomer I, see Figure 1, whereas Table 2 lists some relevant properties of those aggregates. It can be seen from the table that the binding energy increases, whereas the average

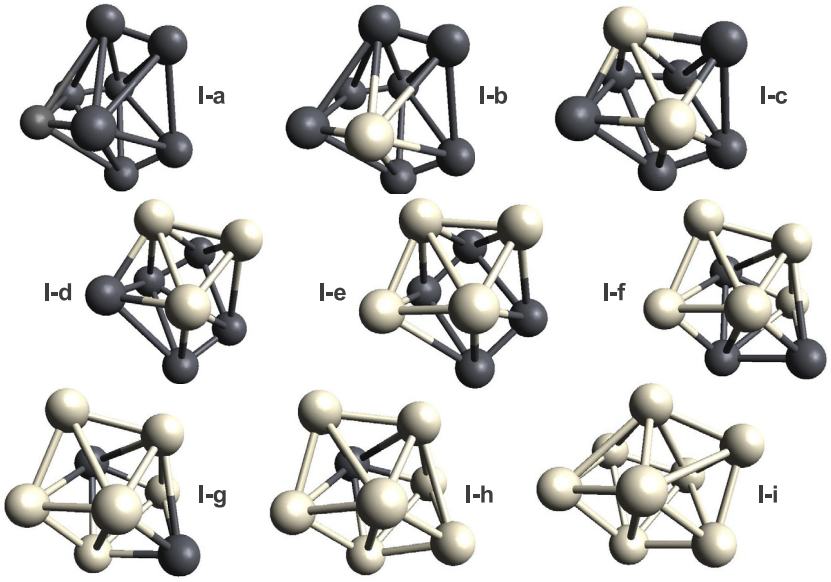

Fig. 2. Optimized structures of the lowest-energy clusters derived from isomer I. Black and white circles represent Mo and W atoms, respectively.

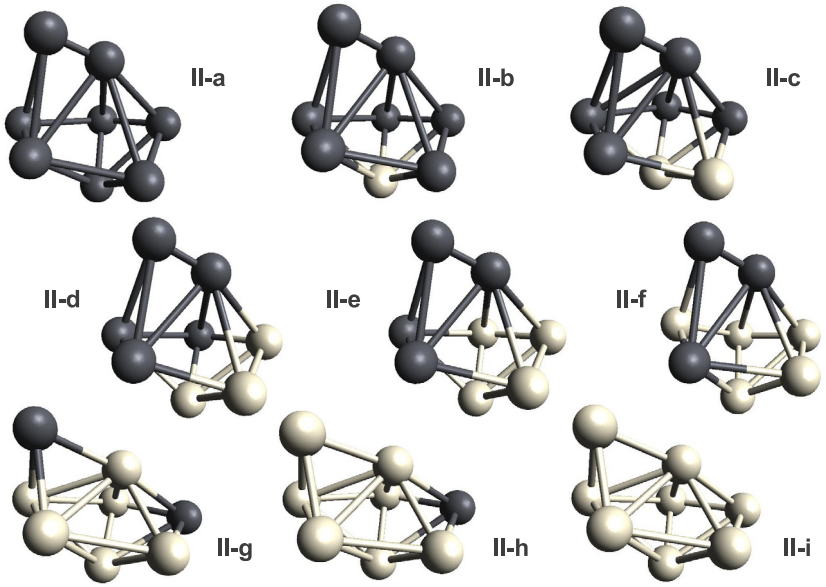

Fig. 3. Optimized structures of the lowest-energy clusters derived from isomer II. Black and white circles represent Mo and W atoms, respectively.

equilibrium distance decreases as the number of W atoms increases in the aggregates. All the aggregates are closed-shell systems and present average coordination numbers that reveal that for those dilute aggregates with up to two atoms of the minor component W atoms tend to form more bonds in general than Mo atoms do. Both the order parameters, σ_{Mo} and σ_{W}, and the drawings in Figure 2 indicate a clear tendency to segregate when W atoms are added to pure Mo_8 replacing Mo atoms. On the other hand, a slight mixing pattern is preferred by Mo atoms when they replace W atoms in W_8, specially in I-f and I-g, for which σ_{Mo} ranges from –0.10 to –0.13.

The optimized structures of the most stable species derived from isomer II, see Figure 1, are depicted in Figure 3. Relevant properties of those isomers are shown in Table 3. A non-negligible structural change can be observed when passing from Mo_3W_5 (II-f) to Mo_2W_6 (II-g). The binding energies show a similar behavior to that observed for isomer I, whereas average equilibrium distances exhibit a smooth decrease in their values when the amount of W atoms increases. Pure aggregates and those clusters with the higher W-content exhibit a triplet electronic state, whereas the remaining clusters show a singlet electronic state. The average coordination numbers indicate again that W atoms form more bonds in general than

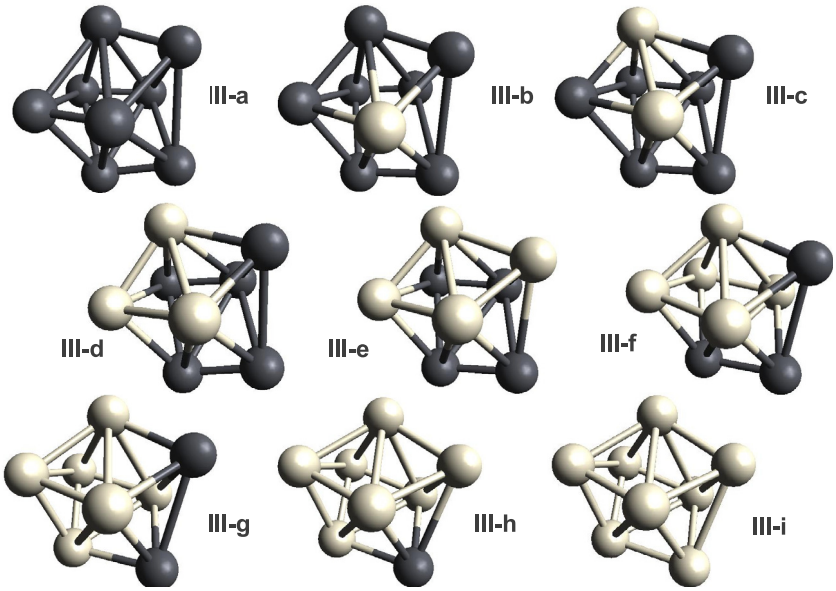

Fig. 4. Optimized structures of the lowest-energy clusters derived from isomer III. Black and white circles represent Mo and W atoms, respectively.

Table 3. Binding energy, E_b in eV/at, order parameters, σ_{Mo} and σ_{W}, average equilibrium distance, R_e^{avg} in Å, average coordination numbers, N_{Mo}^{avg} and N_{W}^{avg}, and magnetic moment, μ in μ_B, for aggregates derived from isomer II, see Figure 1 for the starting geometry and Figure 3 for labels.

Aggregate	E_b	σ_{Mo}	σ_{W}	R_e^{avg}	N_{Mo}^{avg}	N_{W}^{avg}	μ
II-a	–2.768	–	–	2.669	4.25	–	0.25
II-b	–2.996	0.51	–0.03	2.679	4.43	5.00	0.00
II-c	–3.233	0.21	–0.05	2.672	4.50	4.50	0.00
II-d	–3.457	0.16	0.00	2.669	4.60	4.33	0.00
II-e	–3.666	0.13	0.13	2.661	4.75	4.25	0.00
II-f	–3.853	0.00	0.16	2.650	4.67	4.40	0.00
II-g	–4.067	–0.09	0.39	2.620	3.50	5.17	0.25
II-h	–4.289	–0.03	0.63	2.620	4.00	4.86	0.25
II-i	–4.508	–	–	2.622	–	4.75	0.25

Table 4. Binding energy, E_b in eV/at, order parameters, σ_{Mo} and σ_{W}, average equilibrium distance, R_e^{avg} in Å, average coordination numbers, N_{Mo}^{avg} and N_{W}^{avg}, and magnetic moment, μ in μ_B, for aggregates derived from isomer III, see Figure 1 for the starting geometry and Figure 4 for labels.

Aggregate	E_b	σ_{Mo}	σ_{W}	R_e^{avg}	N_{Mo}^{avg}	N_{W}^{avg}	μ
III-a	–2.677	–	–	2.637	4.50	–	0.25
III-b	–2.964	0.48	–0.03	2.630	4.43	5.00	0.25
III-c	–3.219	0.17	–0.06	2.605	4.34	5.00	0.50
III-d	–3.466	0.11	0.00	2.601	4.40	4.67	0.50
III-e	–3.705	0.06	0.06	2.610	4.50	4.50	0.50
III-f	–3.936	–0.08	0.08	2.586	4.34	4.60	0.67
III-g	–4.177	–0.03	0.36	2.585	4.00	4.67	0.67
III-h	–4.410	–0.03	0.58	2.585	4.00	4.57	0.67
III-i	–4.639	–	–	2.584	–	4.50	0.67

Mo atoms do for dilute clusters, as in the case of isomer I. Although the order parameters for diluted clusters present small negative values, a close inspection to Figure 3 clearly shows a tendency to segregate for all the species derived from isomer II, except for aggregate II-g, for which σ_{Mo} is –0.09 and Mo atoms exhibit a tendency to disorder.

The optimized geometries of the most stable species deriving from isomer III, see Figure 1, are shown in Figure 4. Table 4 lists various properties of the optimized species. The binding energies and average equilibrium distances show a similar behavior to that observed for isomer II. Aggregates with high Mo-content exhibit a triplet electronic state, whereas those clusters with high W-content show a septet electronic state. Those clusters with similar Mo- and W-contents are characterized by a quintet electronic state. The average coordination numbers indicate that W atoms tend to form more bonds in general than Mo atoms do for all the compositions studied, except for Mo_4W_4 (III-e), in which the average coordination number of both atoms is the same. The drawings in Figure 4 indicate that there is a clear tendency to segregation in dilute clusters. This finding is supported by the order parameters shown in Table 4 that exhibit very small negative values from –0.08 to –0.03. Interestingly, the comparison of these results with those obtained for isomer II seems to suggest that individual order parameters in the range –0.08––0.09 characterize the transition from segregation to disordered structures.

Figure 5 and Table 5 show the optimized structures and some relevant properties, respectively, of the most stable species derived from isomer IV, see Figure 1. As in the case of isomer II, the binding energies increase their values as the W-content increases. Interestingly, the average equilibrium distance diminishes from IV-a to IV-b

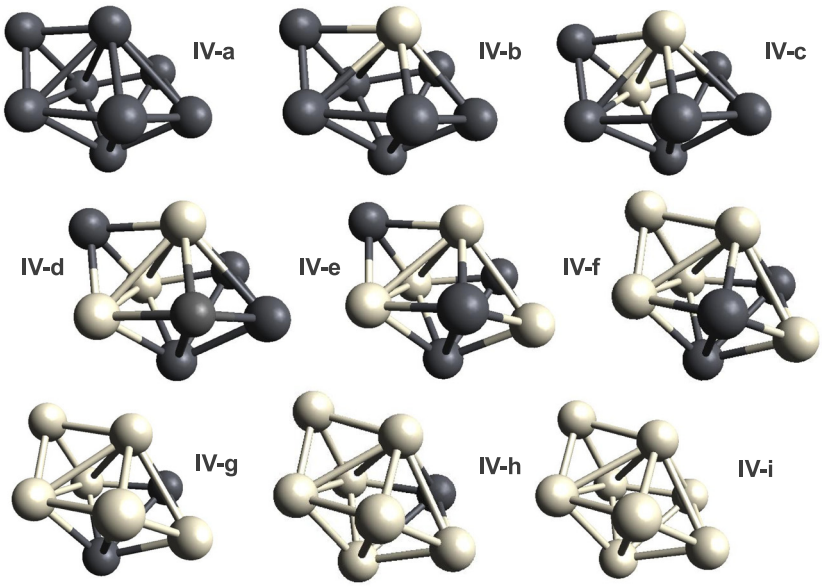

Fig. 5. Optimized structures of the lowest-energy clusters derived from isomer IV. Black and white circles represent Mo and W atoms, respectively.

Table 5. Binding energy, E_b in eV/at, order parameters, σ_{Mo} and σ_{W}, average equilibrium distance, R_e^{avg} in Å, average coordination numbers, N_{Mo}^{avg} and N_{W}^{avg}, and magnetic moment, μ in μ_B, for aggregates derived from isomer IV, see Figure 1 for the starting geometry and Figure 5 for labels.

Aggregate	E_b	σ_{Mo}	σ_{W}	R_e^{avg}	N_{Mo}^{avg}	N_{W}^{avg}	μ
IV-a	–2.653	–	–	2.591	4.50	–	0.25
IV-b	–2.940	0.31	–0.05	2.577	4.29	6.00	0.25
IV-c	–3.212	0.03	–0.08	2.575	4.17	5.50	0.25
IV-d	–3.474	–0.10	–0.06	2.574	4.00	5.33	0.25
IV-e	–3.724	–0.24	–0.13	2.574	4.00	5.00	0.25
IV-f	–3.978	–0.09	0.04	2.575	4.33	4.60	0.25
IV-g	–4.217	–0.05	0.21	2.575	4.50	4.50	0.25
IV-h	–4.452	–0.03	0.61	2.575	4.00	4.57	0.25
IV-i	–4.681	–	–	2.578	–	4.50	0.25

and, then, it remains almost constant up to W_8. The nine species considered are characterized by a triplet electronic state. The average coordination numbers clearly show that W atoms form more bonds in general than Mo atoms do for all the aggregates derived from isomer IV. The individual order parameters show a very interesting behavior, both for Mo and for W. For Mo, aggregates IV-g and IV-h show little tendency to disorder. The σ_{Mo} parameter becomes more negative for IV-f as a consequence of a decrease in the number of Mo-Mo bonds per atom with respect to IV-g. The value of –0.09 indicates a transition to more disordered structures. The number of Mo-Mo bonds per atom decreases even more in IV-e giving rise to an order parameter of –0.24, indicating a strong mixing between Mo and W atoms, see Figure 5. The number of Mo-Mo bonds per atom increases slightly in IV-d and σ_{Mo} becomes less negative, its value still suggesting a rather disordered structure, though. The order parameter for Mo is positive for IV-b and IV-c, mainly due to the high Mo-content in the aggregates. The order parameter for W, on the other hand, shows that W atoms tend to segregate in IV-b, IV-c and IV-d. A lowering in the W-W bonds per atom leads to an order parameter that reveals some trend to disorder in IV-e. Nevertheless, as the W content increases, σ_{W} becomes positive as expected.

Table 6 shows some relevant properties of the most stable species derived from isomer V, see Figure 1, whereas Figure 6 depicts their optimized structures. As expected, the binding energies increase their values as the W-content increases. Interestingly, the average equilibrium distances remain almost constant for all species, the differences being just in the third decimal place. Pure Mo_8 cluster presents a septet electronic state, whereas the remaining species are characterized by a quintet electronic state. The average coordination numbers show that Mo atoms tend to form more bonds in general than W atoms do for all the aggregates derived from isomer V. This is the opposite behavior as the one observed for the structures derived from isomers I to IV. The order parameter for Mo shows an appreciable tendency to disorder in V-g. That trend decreases in V-f and V-e due to the increase in the Mo-Mo bonds per atom, but there is still a tendency to disorder. For the species with high Mo-content the order parameter indicates that segregation is preferred over mixing. A similar behavior is observed for W, notably in V-d and V-e. In the first one, a W atom and a W dimer are completely separated by a Mo sub-cluster, whereas in V-e two W dimers are isolated from each other by a planar Mo_4 sub-cluster, see Figure 6. Order parameters of –0.17 and –0.22 support those observations. Aggregates V-c and V-f also show negative order parameters that suggest that a

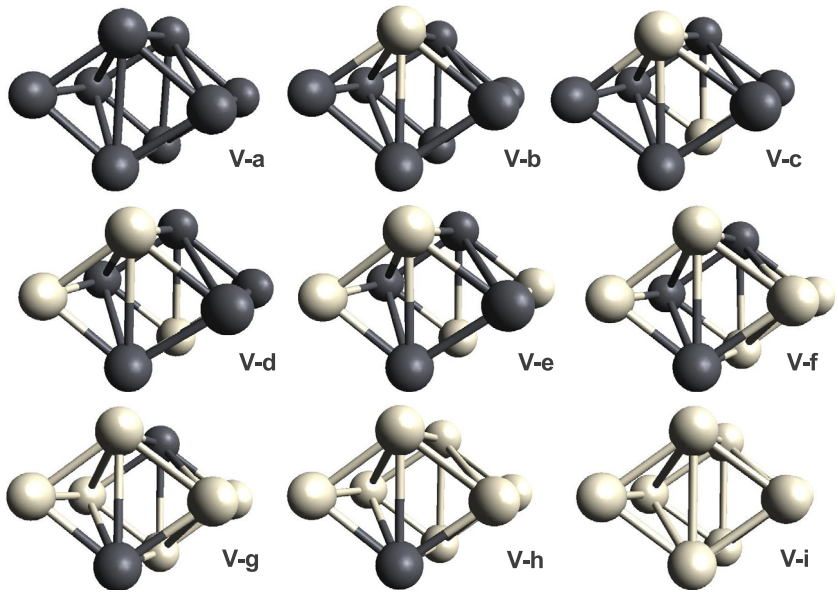

Fig. 6. Optimized structures of the lowest-energy clusters derived from isomer V. Black and white circles represent Mo and W atoms, respectively.

Table 6. Binding energy, E_b in eV/at, order parameters, σ_{Mo} and σ_{W}, average equilibrium distance, R_e^{avg} in Å, average coordination numbers, N_{Mo}^{avg} and N_{W}^{avg}, and magnetic moment, μ in μ_B, for aggregates derived from isomer V, see Figure 1 for the starting geometry and Figure 6 for labels.

Aggregate	E_b	σ_{Mo}	σ_{W}	R_e^{avg}	N_{Mo}^{avg}	N_{W}^{avg}	μ
V-a	–2.603	–	–	2.586	4.50	–	0.67
V-b	–2.883	0.48	–0.03	2.587	4.43	5.00	0.50
V-c	–3.156	0.03	–0.14	2.585	4.34	5.00	0.50
V-d	–3.430	–0.05	–0.17	2.584	4.59	4.34	0.50
V-e	–3.699	–0.11	–0.22	2.583	5.00	4.00	0.50
V-f	–3.958	–0.12	–0.10	2.584	5.00	4.20	0.50
V-g	–4.213	–0.14	0.03	2.583	5.00	4.34	0.50
V-h	–4.453	–0.03	0.48	2.585	5.00	4.43	0.50
V-i	–4.694	–	–	2.586	–	4.50	0.50

rather disordered structure is preferred over an ordered one.

The same information shown in the other tables is gathered in Table 7 for the GS of each composition to ease the comparison between the properties of the lowest-energy clusters. It can be seen in the table that there is a continuous decrease in the average equilibrium distance up to Mo_5W_3 (IV-d) and, then, it remains almost constant with a very slight increase as the W content increases. The average coordination numbers indicate that W atoms present a clear tendency to form more bonds in general than Mo atoms do, specially for low and medium W-contents. Those clusters with high Mo- and W-contents are characterized by singlet and quintet electronic states, respectively, whereas those aggregates with similar contents of the two metals present triplet electronic states. The order parameter for Mo clearly indicates that in the Mo_5W_3 and Mo_4W_4 (IV-e) clusters and, to a lesser extent, the Mo_3W_5 (IV-f) one, Mo atoms tend to form disordered sub-structures. On the other hand, W atoms tend to form segregated structures, the only exception being the Mo_4W_4 aggregate, which exhibits an order parameter of –0.13.

Figure 7 shows two different excess energies and the second difference in the binding energy for the most stable clusters of each composition, see Table 7. The excess energy shown in the lower panel of the figure was obtained using the binding energies of the global GS of Mo_8 and W_8. The excess energy depicted in the middle panel of the figure, on the other hand, was calculated using the binding energies of the pure aggregates of each isomer. It is worth noting that the excess energy in the lower panel shows that no bimetallic system is favored with respect to the global GS of pure clusters, although those aggregates with 5 to 7 W atoms exhibit a small, positive excess energy. However, when the excess energy is calculated with respect to the pure clusters of every isomer, several species become more favored than their pure counterparts, notably those with 3 to 5 W atoms in their composition. The $\Delta_2 E$ function shows that only those aggregates with 2 and 5 W atoms are local maxima, indicating a relative stability with respect to their neighbors.

Figure 8 shows the AIE, the AEA and the global hardness of the most stable clusters of each composition, see Table 7 for more information. The AIE shows an appreciable decrease for those clusters with 3 to 6 W atoms. Then, the ionization energy increases up to its maximum value for W_8. The AEA, on the other hand, decreases when passing from pure Mo_8 to Mo_7W and, next, shows an important increase for Mo_6W_2 remaining almost constant up to achieve its maximum value for W_8. The global hardness suggests that those clusters with 2 to 8 W atoms

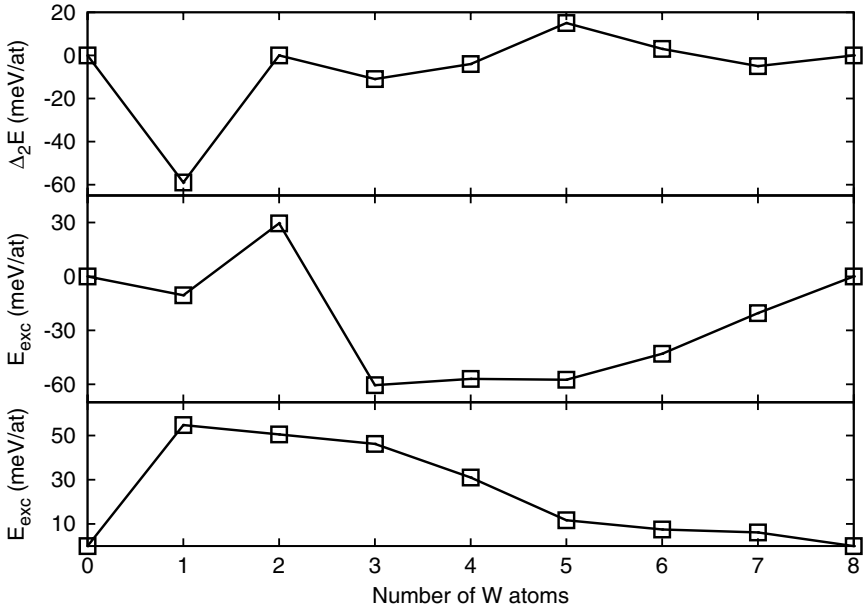

Fig. 7. Excess energy and second difference in the binding energy of the most stable $Mo_{8-q}W_q$ clusters, $q = 0$ to 8, as functions of the number of tungsten atoms. The excess energy in the lower panel was calculated with respect to the global ground states of Mo_8 and W_8. The excess energy in the middle panel was calculated with respect to the Mo_8 and W_8 clusters of each isomer.

Table 7. Binding energy, E_b in eV/at, order parameters, σ_{Mo} and σ_W, average equilibrium distance, R_e^{avg} in Å, average coordination numbers, N_{Mo}^{avg} and N_W^{avg}, and magnetic moment, μ in μ_B, for the lowest-energy aggregates derived from isomers I to V, see Figure 1.

Aggregate	E_b	σ_{Mo}	σ_W	R_e^{avg}	N_{Mo}^{avg}	N_W^{avg}	μ
I-a	–2.816	–	–	2.812	4.50	–	0.00
II-b	–2.996	0.51	–0.03	2.679	4.43	5.00	0.00
I-c	–3.235	0.17	–0.06	2.630	4.33	4.67	0.00
IV-d	–3.474	–0.10	–0.06	2.574	4.00	5.33	0.25
IV-e	–3.724	–0.24	–0.13	2.574	4.00	5.00	0.25
IV-f	–3.978	–0.09	0.04	2.575	4.33	4.60	0.25
IV-g	–4.217	–0.05	0.21	2.575	4.50	4.50	0.25
V-h	–4.453	–0.03	0.48	2.585	5.00	4.43	0.50
V-i	–4.694	–	–	2.586	–	4.50	0.50

should present a similar reactivity pattern against a charge transfer process.

Combining the results shown in Figures 7 and 8, it can be summarized that although Mo_6W_2 and Mo_3W_5 are more stable than their neighbors, the excess energy clearly favors those aggregates with more than three W atoms. Moreover, the global hardness indicates that those clusters with 2 or more W atoms could be good candidates to take part of a charge transfer reaction. Thus, it seems that the Mo_3W_5 aggregate simultaneously fulfills the criteria based on energetic and reactivity indexes and should be the best candidate to participate in a charge transfer reaction like those that occur in hydrotreating processes.

4 Conclusions

The geometric features, electronic and magnetic properties, and reactivity patterns of gas-phase Mo_pW_q atomic clusters, with $p + q = 8$, were investigated within the framework of the generalized gradient approximation to the density functional theory.

Starting from dodecaedral, thin decaedral, decaedral, octahedral and parallelepiped structures for Mo_8 and W_8, all the possible homotops were modeled and their optimized geometries were obtained.

No appreciable distortion in the starting structures was observed when relaxed geometries of the homotops were obtained, except for the transition from Mo_3W_5 to Mo_2W_6 in the thin decaedral form.

It was found that W atoms show an important tendency to segregate for all the structures studied, except for the parallelepiped form, in which an appreciable tendency to generate disordered structures was observed. Mo atoms, on the other hand, exhibit a tendency to form disordered structures when dodecaedral and parallelepiped forms are used as starting points for geometry optimization. When thin decaedral, decaedral and octahedral structures were studied, a clear tendency to segregation was found when Mo atoms replace W atoms.

When the most stable aggregates of each composition were compared, it was found that a singlet electronic state characterize the Mo_8, Mo_7W and Mo_6W_2 species. The Mo_5W_3, Mo_4W_4, Mo_3W_5 and Mo_2W_6 clusters were found to be characterized by a triplet electronic state, whereas MoW_7 and W_8 show a quintet electronic state.

Some stability criteria based on the binding energy indicated that Mo_6W_2 and Mo_3W_5 are relatively more stable than their immediate neighbors. The subset of the

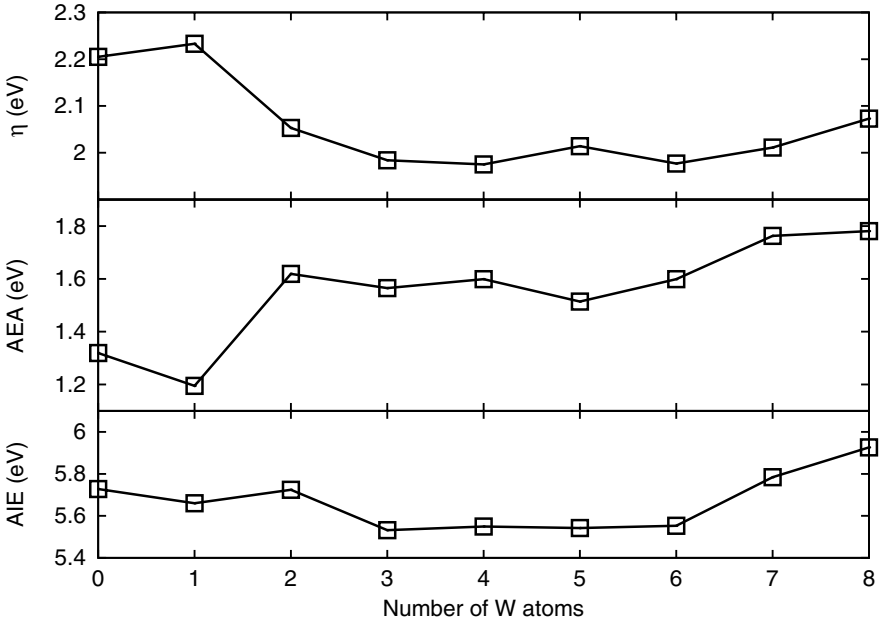

Fig. 8. Adiabatic ionization energy, adiabatic electron affinity and global hardness of the most stable $Mo_{8-q}W_q$ clusters, $q = 0$ to 8, as functions of the number of tungsten atoms.

most stable $Mo_{8-p}W_p$ aggregates, with $3 \leq p \leq 7$, turned out to be more favored than their pure counterparts.

The global hardness suggests that the most stable $Mo_{8-p}W_p$ clusters, with $p \geq 2$, should exhibit the larger reactivity in the whole series.

It is concluded that the Mo_3W_5 aggregate should be a good candidate to take part in a charge transfer reaction, like those observed in hydrodesulfurization and hydrotreating process.

F.A.G. acknowledges financial support from PROMEP-SEP11-CA230 (México) and CONACyT 162651 (México). R.P.D. is member of the Scientific Research Career of CONICET, Argentina. F.A.G. also thanks A. Vega and J.L. Gallego for helpful discussions on the SIESTA code and on the pseudopotentials used in the calculations. The authors also acknowledge J. Limón for computational support.

References

1. J. Bocarando, G. Alonso-Nuñez, W. Bensch, R. Huirache-Acuña, M. Del Valle, J. Cruz-Reyes, Catal. Lett. **130**, 301 (2009)
2. K. Ramanathan, S.W. Weller, J. Catal. **95**, 249 (1985)
3. P.J. Mangnus, A. Bos, J.A. Moulijn, J. Catal. **146**, 437 (1994)
4. J. Espino, L. Alvarez, C. Ornelas, J.L. Rico, S. Fuentes, G. Berhault, G. Alonso, Catal. Lett. **90**, 71 (2003)
5. H.R. Reinhoudt, A.D. Van Langeveld, P.J. Kooyman, R.M. Stockmann, R. Prins, H.W. Zandbergen, J.A. Moulijn, J. Catal. **179**, 443 (1998)
6. Y. Yoshimura, T. Sato, H. Shimada, N. Matsubayashi, M. Imamura, A. Nishijima, M. Higo, S. Yoshitomi, Catal. Today **29**, 221 (1996)
7. S.I. Woo, C.H. Kim, W.L. Yoon, I.C. Lee, Appl. Catal. A Gen. **144**, 159 (1996)
8. D.K. Lee, H.T. Lee, I.C. Lee, S.K. Park, S.Y. Bae, C.H. Kim, S.I. Woo, J. Catal. **159**, 219 (1996)
9. D.K. Lee, I.C. Lee, S.K. Park, S.Y. Bae, S.I. Woo, J. Catal. **159**, 212 (1996)
10. J. Vakros, C. Kordulis, Appl. Catal. A Gen. **217**, 287 (2001)
11. H. Nava, F. Pedraza, G. Alonso, Catal. Lett. **99**, 65 (2005)
12. R. Huirache-Acuña, M.A. Albiter, C. Ornelas, F. Paraguay-Delgado, R. Martínez-Sánchez, G. Alonso-Nuñez, Appl. Catal. A Gen. **208**, 134 (2006)
13. A. Olivas, D.H. Galván, G. Alonso, S. Fuentes, Appl. Catal. A Gen. **352**, 10 (2009)
14. *Theory of Atomic and Molecular Clusters*, edited by J. Jellinek (Springer, Berlin, 1999)
15. R.L. Johnston, *Atomic and Molecular Clusters* (Taylor and Francis, London, 2002)
16. E.K. Parks, B.J. Winter, T.D. Klots, S.J. Riley, J. Chem. Phys. **94**, 1882 (1991)
17. E.K. Parks, B.J. Winter, T.D. Klots, S.J. Riley, J. Chem. Phys. **96**, 8267 (1992)
18. E.K. Parks, L. Zhu, J. Ho, S.J. Riley, J. Chem. Phys. **100**, 7206 (1994)
19. E.K. Parks, L. Zhu, J. Ho, S.J. Riley, J. Chem. Phys. **102**, 7377 (1995)
20. E.K. Parks, K.P. Kerns, S.J. Riley, Chem. Phys. **262**, 151 (2000)
21. R. Pis-Diez, Int. J. Quantum Chem. **76**, 105 (2000)
22. F. Aguilera-Granja, A. Vega, J.L. Gallego, Nanotechnology **19**, 145704 (2008)
23. Z.J. Wu, Chem. Phys. Lett. **370**, 510 (2003)
24. W. Yamaguchi, J. Murakami, Chem. Phys. **316**, 45 (2005)

25. J. Du, X. Sun, D. Meng, P. Zhang, G. Jiang, J. Chem. Phys. **131**, 044313 (2009)
26. S.M. Carrión, R. Pis-Diez, F. Aguilera-Granja, Eur. Phys. J. D **67**, 3 (2013)
27. J.M. Soler, E. Artacho, J.D. Gale, A. García, J. Junquera, P. Ordejón, D. Sánchez-Portal, J. Phys.: Condens. Matter **14**, 2745 (2002)
28. N. Troullier, J.L. Martins, Phys. Rev. B **43**, 1993 (1991)
29. L. Kleinman, D.M. Bylander, Phys. Rev. Lett. **48**, 1425 (1982)
30. J.P. Perdew, K. Burke, M. Ernzerhof, Phys. Rev. Lett. **77**, 3865 (1996)
31. W.H. Press, S.A. Teukolsky, W.T. Vetterling, B.P. Flannery, *Numerical Recipes in Fortran*, 2nd edn. (Cambridge University Press, Cambridge, 1992)
32. R. Ferrando, J. Jellinek, R.L. Johnston, Chem. Rev. **108**, 845 (2008)
33. R.G. Parr, W. Yang, *Density Functional Theory of Atoms and Molecules* (Oxford University Press, 1989)
34. F. Ducastelle, *Order and Phase Stability in Alloys* (North-Holland, Amsterdam, 1991)
35. M.D. Morse, Chem. Rev. **86**, 1049 (1986)
36. J.R. Lombardi, B. Davis, Chem. Rev. **102**, 2431 (2002)